Short Papers

Reference Frames Fit for Controlling PWM Rectifiers

J. L. Duarte, A. van Zwam, C. Wijnands, and A. Vandenput

***Abstract*—Keep things simple when controlling bidirectional pulsewidth modulation rectifiers by considering the utility grid as a virtual electric machine. The advantage is that the air-gap flux of this big machine can be directly measured in a straightforward way. Therefore, as shown in this paper, principles of field orientation can be applied to control the power flow, yielding high-dynamic performance.**

***Index Terms*—Active filters, field-oriented control, power quality.**

I. Introduction

The integration of the utility grid voltages with respect to time yields a virtual rotating magnetic-flux vector which can be chosen as a privileged reference frame to control bidirectional pulsewidth modulation (PWM) rectifiers. The projection of the system equations onto this rotating frame leads to the separation of the line current into two orthogonal components. The component in quadrature with the virtual-flux vector imposes the instantaneous active-power exchange, while the direct-axis component gives the instantaneous reactive power between the phases. As a consequence, decoupled and high-dynamic power control is made possible, in complete similarity with well-known techniques commonly applied to electrical machines.

II. System Description Based on Virtual-Flux Orientation

To put the main control issues into perspective, a diagram of a PWM-rectifier system is shown in Fig. 1. The principles of field orientation can be readily adopted for describing the system behavior, if the voltages imposed by the utility grid in combination with the ac-side inductors are assumed to be quantities related to a virtual ac machine. With this abstraction in mind, L_σ and R_σ represent the stator leakage inductance and the stator resistance of the virtual machine, respectively. Hence, the phase-to-phase grid voltages u_{ab}, u_{bc}, u_{ca} would be induced by a virtual air-gap flux. Otherwise stated, the integration of the phase-to-phase grid voltages leads to a virtual grid-flux vector $\mathbf{\Psi}_g$, which is rotating with respect to a stationary frame oriented with the machine stator. Thus, according to the definitions in the Appendix,

$$\mathbf{\Psi}_g^s = \begin{bmatrix} \psi_g^{s1} \\ \psi_g^{s2} \end{bmatrix} = \int \mathbf{u}_g^s \, dt = \begin{bmatrix} \int u_g^{s1} \, dt \\ \int u_g^{s2} \, dt \end{bmatrix}. \tag{1}$$

Consequently, with regard to the stator frame, the relationship between stator voltage, stator current, and stator flux at the terminals A, B, C in Fig. 1 is found to be

$$\mathbf{u}_s^s = R_\sigma \imath_s^s + \frac{d}{dt}\mathbf{\Psi}_s^s, \qquad \text{with } \mathbf{\Psi}_s^s = L_\sigma \imath_s^s + \mathbf{\Psi}_g^s. \tag{2}$$

Manuscript received October 3, 1997; revised November 15, 1998. Abstract published on the Internet March 1, 1999.

J. L. Duarte and A. Vandenput are with the Electromechanics and Power Electronics Group, TU Eindhoven, 5600 MB Eindhoven, The Netherlands (e-mail: j.l.duarte@tue.nl).

A. van Zwam and C. Wijnands are with Prodrive BV, 5692 EB Son, The Netherlands (e-mail: KW@prodrive.nl).

Publisher Item Identifier S 0278-0046(99)04144-1.

The angular displacement of $\mathbf{\Psi}_g$ with reference to the stator frame, φ_g^s, is then

$$\cos\,\varphi_g^s = \psi_g^{s1}/\psi_g, \qquad \sin\,\varphi_g^s = \psi_g^{s2}/\psi_g \tag{3}$$

where $\psi_g = \sqrt{\left(\psi_g^{s1}\right)^2 + \left(\psi_g^{s2}\right)^2}$. Thereby, the radian frequency $\omega = d\varphi_g^s/dt$ is as follows:

$$\omega = \frac{1}{(\psi_g)^2}\left(\psi_g^{s1}\frac{d}{dt}\psi_g^{s2} - \psi_g^{s2}\frac{d}{dt}\psi_g^{s1}\right) \tag{4}$$

where ω equals the angular frequency of the ac mains only in the case of symmetric and sinusoidal voltage supply.

The instantaneous active-power flow into the grid, $P_g = \{\mathbf{u}_g^s\}^\top\{\imath_s^s\}$, is found to be, after projection onto a frame oriented with $\mathbf{\Psi}_g$

$$P_g = \frac{d}{dt}\{\psi_g\}\imath_s^{\psi g1} + \omega\psi_g\imath_s^{\psi g2} \tag{5}$$

where the current coordinate transformation is given by

$$\begin{bmatrix} \imath_s^{\psi g1} \\ \imath_s^{\psi g2} \end{bmatrix} = \begin{bmatrix} \cos\,\varphi_g^s & \sin\,\varphi_g^s \\ -\sin\,\varphi_g^s & \cos\,\varphi_g^s \end{bmatrix}\begin{bmatrix} \imath_s^{s1} \\ \imath_s^{s2} \end{bmatrix}. \tag{6}$$

Equation (5) is always valid, even under transients or asymmetric mains voltage. Purely sinusoidal and symmetric supply yields $d\psi_g/dt \equiv 0$. In this case, (5) reduces then to

$$P_g = \omega\psi_g\imath_s^{\psi g2} \tag{7}$$

which means that only the current component in quadrature with $\mathbf{\Psi}_g$ imposes the instantaneous active-power flow.

In order to derive a linear transfer function for the system, it is assumed further that, for simplicity, the line currents are accurately controlled with any method such that $\imath_s^{\psi g1} \equiv 0$, aiming at energy transfer with minimum current and unity power factor. This also means that (7) applies. By taking now the total instantaneous energy stored in the line inductors L_σ into consideration, the power balance of the dc link in Fig. 1, which is buffered by a lossless capacitor $C_{\rm dc}$, is found to become

$$\frac{d}{dt}\left\{\tfrac{1}{2}\,C_{\rm dc}(u_{\rm dc})^2\right\} = P_{\rm Load} - P_g - \frac{d}{dt}\left\{\tfrac{1}{2}\,L_\sigma\left(\imath_s^{\psi g2}\right)^2\right\} \tag{8}$$

with $P_{\rm Load}$ representing the power coming from the downstream converter (for simplicity, the dissipation in R_σ and in the switching transistors is supposed to be negligible). Assuming next small variations in (8), for instance, $\Delta u_{\rm dc} = u_{\rm dc} - [u_{\rm dc}]_0$, where $[u_{\rm dc}]_0$ represents an operating point constant value, etc., the following linearized transfer function results:

$$\Delta u_{\rm dc}(\mathcal{S}) = -\kappa\frac{1+T_1\mathcal{S}}{\mathcal{S}C_{\rm dc}}\,\Delta\imath_s^{\psi g2}(\mathcal{S}) + \frac{1}{\mathcal{S}C_{\rm dc}[u_{\rm dc}]_0}\,\Delta P_{\rm Load}(\mathcal{S}) + u_{\approx}(\mathcal{S}) \tag{9}$$

with $T_1 = L_\sigma[\imath_s^{\psi g2}]_0/[\omega\psi_g]_0$, $\kappa = [\omega\psi_g]_0/[u_{\rm dc}]_0$, and $\mathcal{S}$ denotes the complex Laplace variable. As can be seen from (9), the system has a zero in the right-$\mathcal{S}$-half plane in rectifying mode ($[\imath_s^{\psi g2}]_0 < 0$). For the sake of completeness, in connection with the dimensioning of the dc-link voltage controller, a pertubation input, $u_{\approx}$, has been added to (9), which represents the low-frequency ripple in the dc link that is generated by grid voltage asymmetries [3].

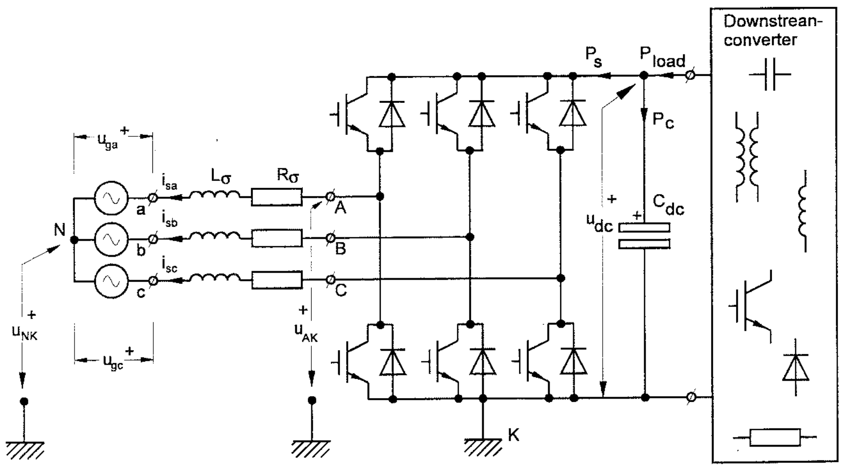

Fig. 1. Structure of a three-phase bidirectional PWM rectifier system. In order to assure proper converter operation, it is necessary to place inductors between the bridge and the utility grid (terminals A, B, C and a, b, c, respectively).

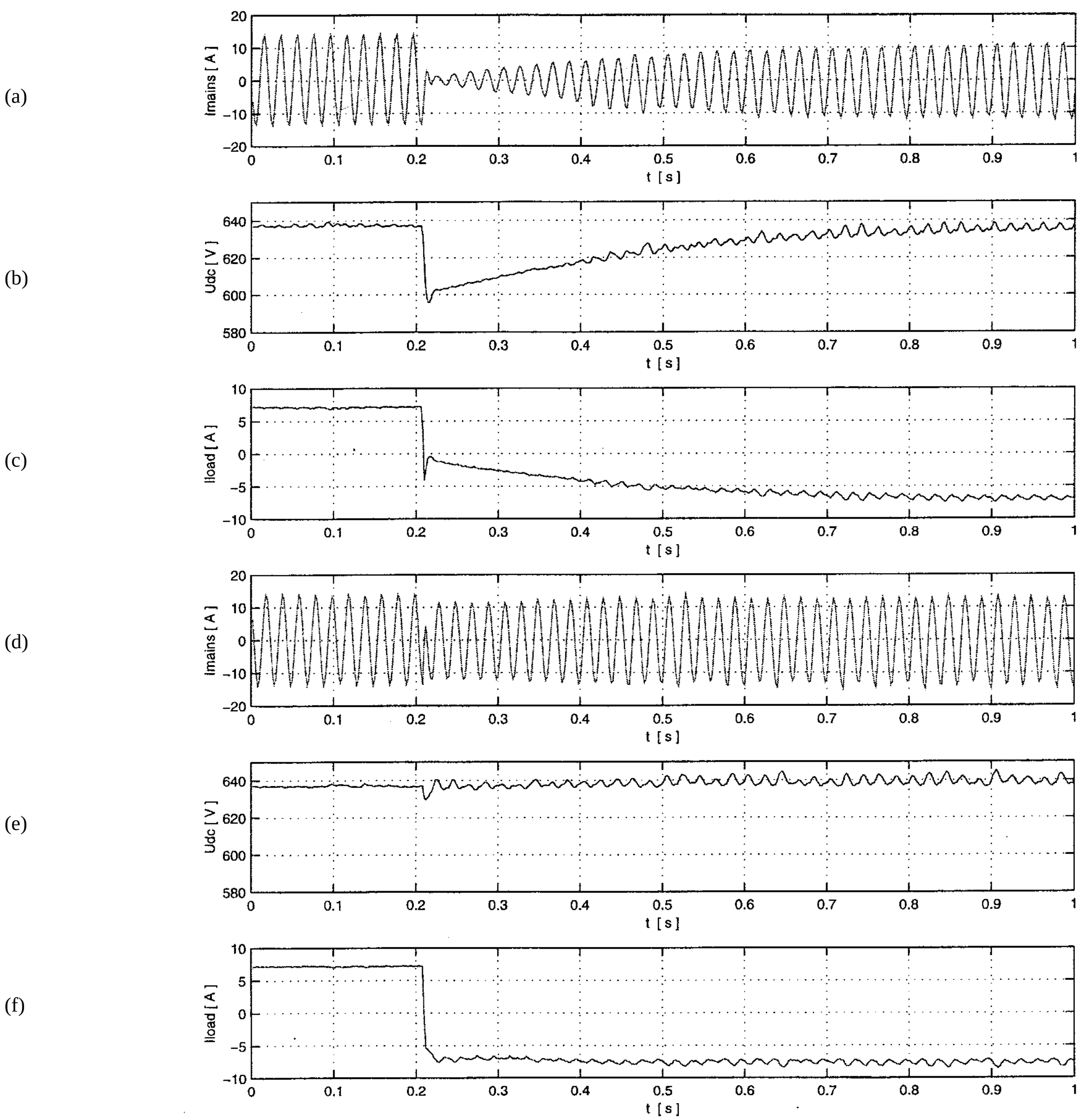

Fig. 2. Experimental results from a 10-kVA/650-Vdc insulated-gate-bipolar-transistor-based PWM-rectifier prototype operating at 5-kHz switching frequency. (a) Line current, (b) dc-link voltage, and (c) load current during a fast transition from rectifying to inverting operation without load feedforward; (d) line current, (e) dc-link voltage, and (f) load current during a fast transition from rectifying to inverting operation with load feedforward.

III. Final Remarks

Conventionally, the analysis of PWM-rectifier systems has been made by splitting the line current into components with respect to the grid voltage [2]. In this case, the angle of the voltage vector with reference to a stationary frame, ϵ_g^s, where

$$\cos\,\epsilon_g^s = u_g^{s1}\Big/\sqrt{\left(u_g^{s1}\right)^2 + \left(u_g^{s2}\right)^2}$$
$$\sin\,\epsilon_g^s = u_g^{s2}\Big/\sqrt{\left(u_g^{s1}\right)^2 + \left(u_g^{s2}\right)^2} \qquad (10)$$

gives the basis for the coordinate transformations. It is clear from (10) that the disturbances superimposed onto the grid voltage influence directly the coordinate projections, therefore, they spread out through the entire control system. Hence, phase-locked loops (PLL's) are usually applied to track the voltage vector in a damped manner. Consequently, the quality of the controlled system depends on how effectively the PLL's have been designed to accomplish this task.

As shown previously, the angle φ_g^s in (3) gives the basis for the flux-oriented approach. Obviously, φ_g^s is less sensitive than ϵ_g^s to disturbances in the grid voltage, on account of the natural low-pass behavior of the integrators in (1) (because nth harmonics are reduced by a factor $1/n$ and the ripple related to the high-frequency transistor switching is strongly damped). For this reason, it is not necessary to implement PLL's to achieve robustness in the flux-oriented scheme, since $\mathbf{\Psi}_g^s$ rotates much more smoothly than $\mathbf{u}_g^s$. Therefore, it is easier to obtain φ_g^s as compared to ϵ_g^s.

The ideas above have been successfully tested on a 10-kVA laboratory prototype. Of course, $\mathbf{\Psi}_g^s$ cannot be derived in practice from an open-loop integration as in (1). Instead, a scheme based on opamps with transfer function

$$\mathbf{\Psi}_g^s(\mathcal{S}) = \frac{\mathcal{S}\tau_a}{(\mathcal{S}\tau_b + 1)(\mathcal{S}\tau_c + 1)}\,\mathbf{u}_g^s(\mathcal{S}) \qquad (11)$$

has been used, providing a large gain around 1 Hz, but zero gain at dc, which mimics a "pure" integrator adequately for all frequencies above 5 Hz. Then, the resulting signals were sampled by a Timex C40-DSP development system to implement further the flux-oriented discrete controllers [4]. A control structure in cascade form has been applied: an inner loop to shape the line currents according to the desired field-oriented components, the quadrature component being given by an outer dc-link voltage control loop, together with feedforward techniques to allow faster transient responses [2]. To perform line-current regulation, the approach in [1] has been adopted. Fig. 2 shows some experimental results.

Appendix
Vector Definitions

$$\mathbf{u}_g^s = \begin{bmatrix} u_g^{s1} \\ u_g^{s2} \end{bmatrix} = \sqrt{2/3}\begin{bmatrix} 1 & 1/2 \\ 0 & \sqrt{3}/2 \end{bmatrix}\begin{bmatrix} u_{ab} \\ u_{bc} \end{bmatrix}$$

$$\mathbf{u}_s^s = \begin{bmatrix} u_s^{s1} \\ u_s^{s2} \end{bmatrix} = \sqrt{2/3}\begin{bmatrix} 1 & -1/2 & -1/2 \\ 0 & \sqrt{3}/2 & -\sqrt{3}/2 \end{bmatrix}\begin{bmatrix} u_{AK} \\ u_{BK} \\ u_{CK} \end{bmatrix}$$

$$\imath_s^s = \begin{bmatrix} \imath_s^{s1} \\ \imath_s^{s2} \end{bmatrix} = \sqrt{2/3}\begin{bmatrix} 3/2 & 0 \\ \sqrt{3}/2 & \sqrt{3} \end{bmatrix}\begin{bmatrix} \imath_{sa} \\ \imath_{sb} \end{bmatrix}$$

with

$$\imath_{sa} + \imath_{sb} + \imath_{sc} \equiv 0.$$

References

[1] T. G. Habetler, "A space vector-based rectifier regulator for AC/DC converters," in *Proc. EPE Conf.*, Florence, Italy, 1991, vol. 2, pp. 101–107.

[2] J. W. Kolar *et al.*, "Analysis of the control behavior of a bidirectional three-phase PWM rectifier system," in *Proc. EPE Conf.*, Florence, Italy, 1991, vol. 2, pp. 95–100.

[3] S. Kalachnikov and H. Berger, "A new control strategy for DC-link voltage of a three-phase bi-directional PWM rectifier," in *Proc. EPE Conf.*, Seville, Spain, 1995, vol. 2, pp. 558–561.

[4] P. J. M. Smidt and J. L. Duarte, "An unity power factor convertor without current measurement," in *Proc. EPE Conf.*, Seville, Spain, 1995, vol. 3, pp. 275–280.